

The Effect of Pressure on Grain Boundary Wetting, Segregation and Diffusion

W. Lojkowski^{1,2}, E. Rabkin³, B. Straumal^{3,4}, L.S. Shvindlerman⁴ and W. Gust³

¹ High Pressure Research Center, Polish Academy of Sciences,
Sokolowska 29, PL-01-142 Warsaw, Poland

² University of Ulm, Department of Electric and Magnetic Materials, Ulm, Germany

³ Institut für Metallkunde, University of Stuttgart, Seestr. 75, D-70174 Stuttgart, Germany

⁴ Institute of Solid State Physics, Russian Academy of Sciences,
Chernogolovka, Moscow District, 142432 Russia

Keywords: Grain Boundary Energy, Diffusion, Segregation, Solid/Liquid Interface, Wetting

Abstract. Grain boundary (GB) wetting involves several phenomena: interaction of two solid/liquid (S/L) interfaces and the GB, diffusion of the elements from the wetting liquid along the GB, phase transformations at the GB, diffusion in the bulk and in the melt near the triple junction of interfaces. High pressure influences all the above phenomena. In the present paper recent results of the study of the pressure effect on the GB wetting phenomenon are reviewed. The main results are: discovery of the pressure induced GB - wetting/dewetting transition, confirmation that during GB wetting by liquid Zn in Fe-6 at.% Si bicrystals GB premelting occurs, description of the solidification of GB at high temperatures, the melting iceberg model of the solid/liquid interface, describing reactive interfaces between the solid and melt.

Introduction. The grain boundary (GB) wetting is a complex phenomenon involving the thermodynamics, kinetics and structure of the GB and solid/liquid (S/L) interfaces, as well as various diffusion mechanisms [1-48]. Its technological importance was established long ago [38-48] and its effect on embrittlement and reliability of materials attracts continuous attention [44]. The purpose of the present paper is to focus attention on the new information following from high pressure studies of the wetting phenomenon [24-28, 34-36]. Firstly, however, a brief review of the phenomena related to GB wetting is given.

Systematics of the Grain Boundary Wetting Phenomena. GB wetting takes place at the intersection of a GB and the solid/liquid (S/L) interface. The crucial parameter is the wetting angle θ (Fig. 1). One can distinguish two cases: a wetting angle $\theta > 0$ (partial wetting) and $\theta = 0$ (wetting). The transition from $\theta > 0$ to $\theta = 0$ is called the wetting transition. Further, one can consider the case when the metal is wetted by its own melt or when it is wetted by another metal. For the case of wetting by the own melt, the liquid and the solid can coexist only in a temperature gradient. When the temperature increases, the liquid penetrates along the GBs. For metals with a high heat of fusion the wetting angle usually depends on whether the temperature is increased or decreased and whether the liquid is an inclusion in the solid phase or is present on the external surface of the solid [2, 45]. The reason is that in metals with a high energy of melting the S/L interface is sharp and has a tendency to facet [45] whereas in metals with low energy of melting the S/L interface is smooth and a few atomic diameters thick [45-49].

Since the melting phenomena take place within a fraction of a degree around the melting point and the temperature in a real system always either increases or decreases, it is difficult to draw

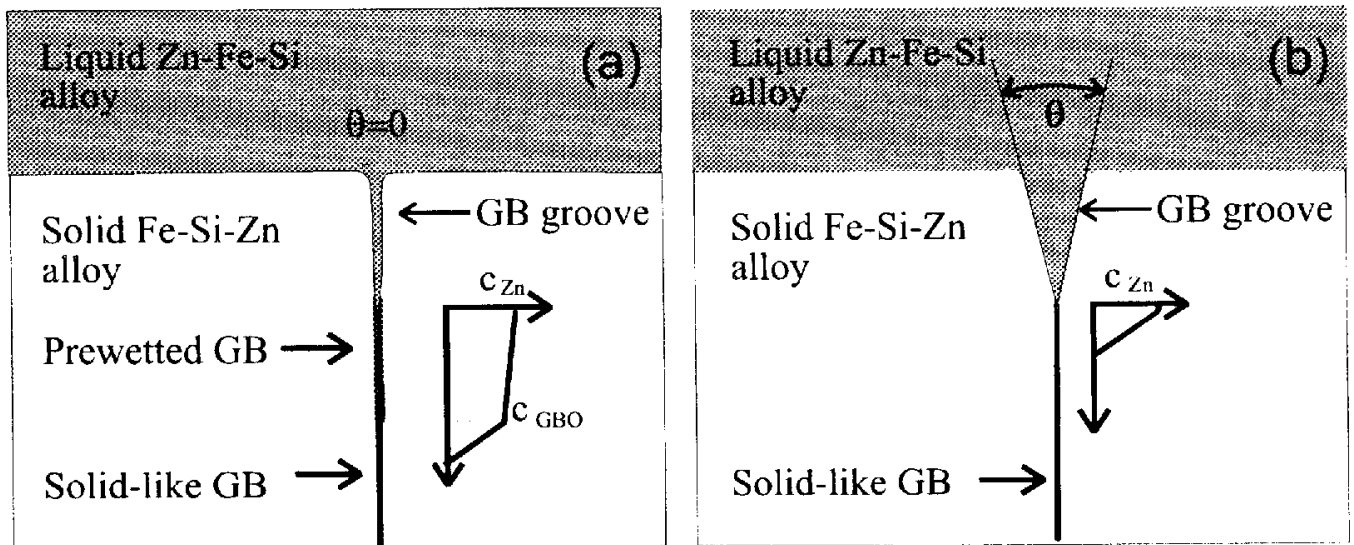


Figure 1. Schematic representation of the wetting angle θ , wetting transition and prewetted GB region on the example of Fe-6at%Si bicrystals wetted by liquid Zn. (a) The GB is wetted and there is a prewetted region of the GB. (b) No prewetting and wetting.

conclusions about the wetting angle for the case of melting of a pure metal. However, one fact seems well established: for low angle GBs $\theta > 0$ while for general GBs $\theta = 0$ [2,50,61]. The practical consequence is that during melting the liquid phase appears first at general GBs. This phenomenon was explained in two ways. One theory is that GBs melt at lower temperatures than the bulk [47].

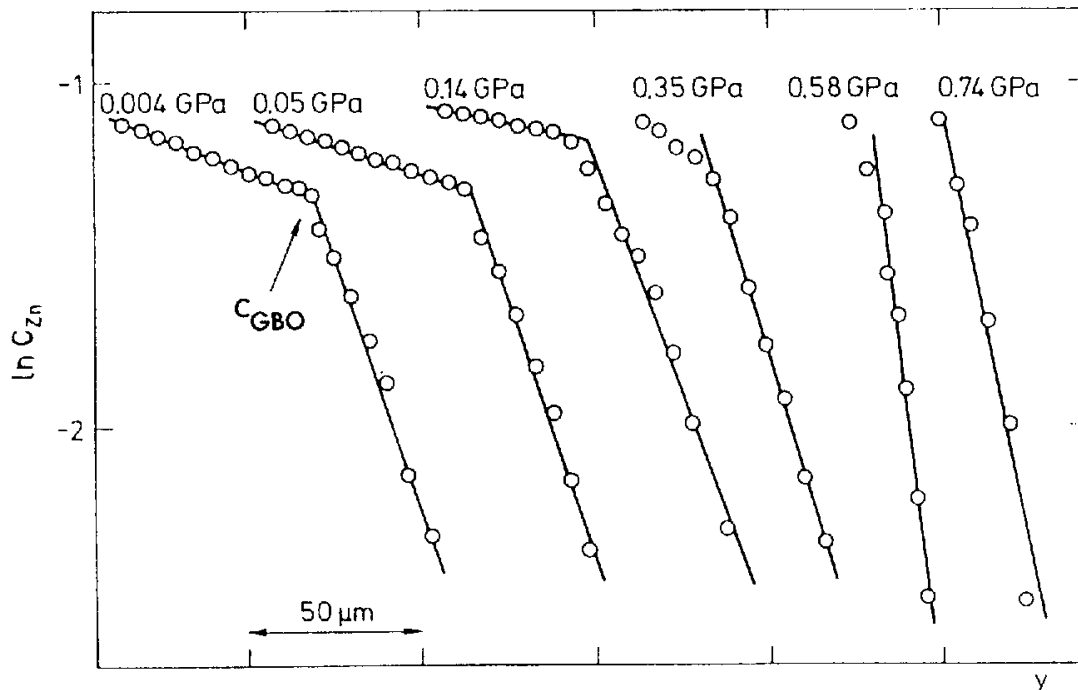


Figure 2. The effect of pressure on the penetration profiles for Zn diffusion along a $43^\circ\langle 001 \rangle$ symmetrical tilt GB in a Fe - 6 at.% Si bicrystal at 905°C . c_{zn} is the measured close to the GB Zn

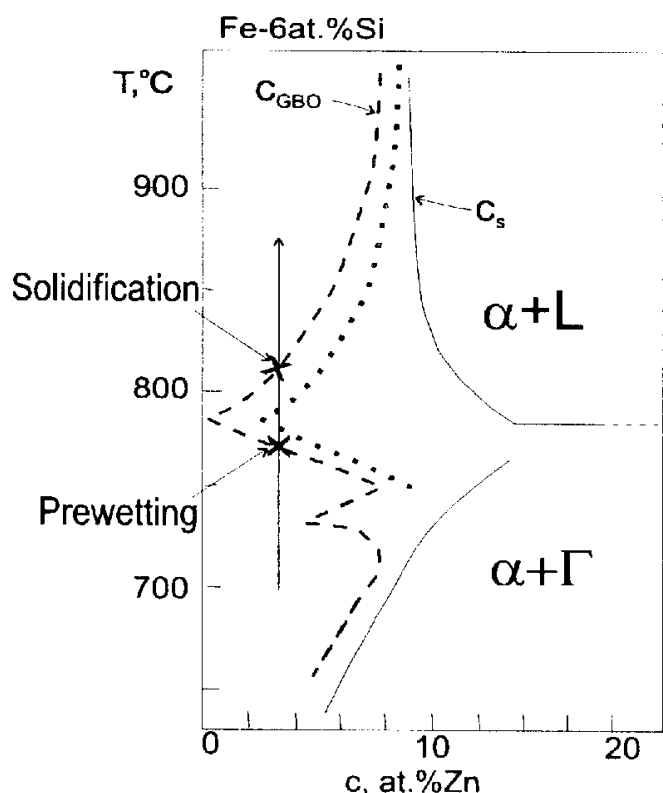


Figure 3. Part of the bulk (solid lines) and GB phase diagram (broken lines) a $45^\circ[001]$ GB in a Fe-6 at.% Si alloy wetted by Zn (according to Rabkin et al [20]). The dashed line shows the GB solubility limit of Zn. The dotted line shows the direction of the shift of the solubility limit under pressure [26,35]. The effect of Si on the phase diagram was neglected. c_{GBO} is defined as the concentration of Zn in the bulk close to the GB above which the GB wetting and pre-melting transition takes place. The lowest c_{GBO} value is for the peritectic temperature. The small cusp at 740°C is connected with the Curie point.

concentration. c_{GBO} is the Zn solubility limit. At c_{GBO} Zn concentration the diffusion rate decreases by two orders of magnitude [24].

According to the calculations of Hillard and Cahn [47], in noble metals the energy of two S/L interfaces is lower than the energy of a GB at the melting point. Therefore, close to the melting point the GB may transform in a sandwich structure with two S/L interfaces separated by a thin layer of undercooled liquid. This phenomenon was called GB premelting and was observed during computer simulations of GBs [51–54]. There is a number of experiments which seem to support this theory [2, 55–57]. However, there are also observations that do not match the premelting theory [50, 58–60]. It was shown during sintering experiments of single crystalline spheres to single crystal surfaces that the spheres rotate to minimize the GB energy even at temperatures 0.95 and 0.97 of the melting point [59, 60]. Further, structural grain boundary dislocations can be observed up to the melting point [58]. The wetting angle is above zero also for low angle boundaries in the case of melting of gallium [61]. The in situ transmission electron microscopy observations of melting of aluminum by Hsieh and Balluffi [50] are not consistent with the premelting theory.

The alternative explanation is that GB premelting is a kinetic phenomenon and GBs are places where melting starts.

One can clearly distinguish two cases of the wetting transition. One is when a very rapid penetration of the GBs by the liquid metal is observed. The mechanism of such a rapid penetration is not clear. The other situation is when the kinetics of the wetting transition is controlled by diffusion and is slow enough to permit investigations of its mechanism. For the systems: Ni wetted by Bi [5], Fe-Si alloys wetted by Zn [20] and Al wetted by Ga [63] the kinetics of GB wetting was studied in detail. It was shown that the low melting point metal diffuses along GBs and transforms their structure. The transformed GBs are characterized by high diffusion coefficients. This transformation was called prewetting transition [20]. For the Fe-Si alloys wetted by Zn it was proposed that the concentration

level of Zn at which the prewetting transition takes place is equivalent to the GB solubility limit of Zn [20]. Let us denote as c_{Zn} the concentration of Zn in the GB. The pre-wetting transition was interpreted as the result of $c_{Zn} > c_{GB0}$, where c_{GB0} is the solubility limit of Zn in the GBs. c_{GB0} is the concentration of Zn in the bulk close to the GB and is measured by estimating the limit value of the Zn concentration when approaching the scanning electron microscope probe to the GB. Detailed investigations of c_{GB0} as a function of the Si content, GB misorientation, temperature and pressure permitted to construct the first GB phase diagrams for the prewetting transition [20, 27] (Fig. 2–4). As far as the physical nature of the prewetting transition, it was assumed that at high c_{Zn} values a thin Zn rich liquid film is present at the GBs which would be unstable outside the GB for the same composition and temperature. In other words, GB premelting is a preliminary stage before GB wetting by the bulk melt. Figure 2 and 3 shows that the solubility limit of Zn in the GBs is the mirror reflection of its solubility in the bulk. Under equilibrium conditions the contact angle θ at the intersection of the GB and the S/L interface (Fig. 1b) is defined by the equation:

$$\cos \frac{\theta}{2} = \frac{\gamma_{GB}}{2\gamma_{SL}}, \quad (1)$$

where γ_{GB} and γ_{SL} are the GB and S/L interface energy per unit area, respectively. The anisotropy of the S/L interface and GB energy is neglected. It is clear that the wetting transition means that:

$$\gamma_{GB} \geq 2\gamma_{SL}. \quad (2)$$

Let us assume that γ_{GB} and γ_{SL} are linear functions of temperature or pressure. Figure 5 and Eq. 3 show that the wetting pressure or temperature shall depend on the energy, excess entropy and excess volume of each of the interfaces.

$$\frac{\theta}{2} = \arccos \left(\frac{\gamma_{GB0} - s_{GB}T + pV_{GB}}{2\gamma_{SLO} - 2s_{SL}T + 2pV_{SL}} \right), \quad (3)$$

where γ_{GB0} and γ_{SLO} are the energies of the GB and S/L interface at zero pressure and room temperature, respectively, s_{GB} and s_{SL} are the excess entropies, V_{GB} and V_{SL} are the excess volumes of the interfaces, and p is the pressure [23–27, 72].

High Pressure Studies of Grain Boundary Wetting. The pressure effect on GB wetting in Fe–6 at.% Si bicrystals wetted by liquid Zn was presented in detail in refs [24–27]. The main results of the high pressure studies are:

(a) *Pressure induced dewetting transition.* It was observed that high pressure prevents GB wetting (Fig. 6). To explain this result it was assumed that the energy of the liquid film penetrating along the GBs during the prewetting transition is increasing faster with increasing pressure than the GB energy (Fig. 5).

(b) *The effect of temperature on the dewetting transition pressure.* It was found that the dewetting pressure is a function of temperature [25] and has a minimum at 885°C (Fig. 7). This result was interpreted in terms of the pressure effect on the Zn solubility limit in GBs. Figure 3 shows the proposed shift of the solubility limit under pressure [26, 35, 36]. At low pressure, wetting occurs at each temperature. However, at high pressure there is a temperature range where the dewetting transition takes place.

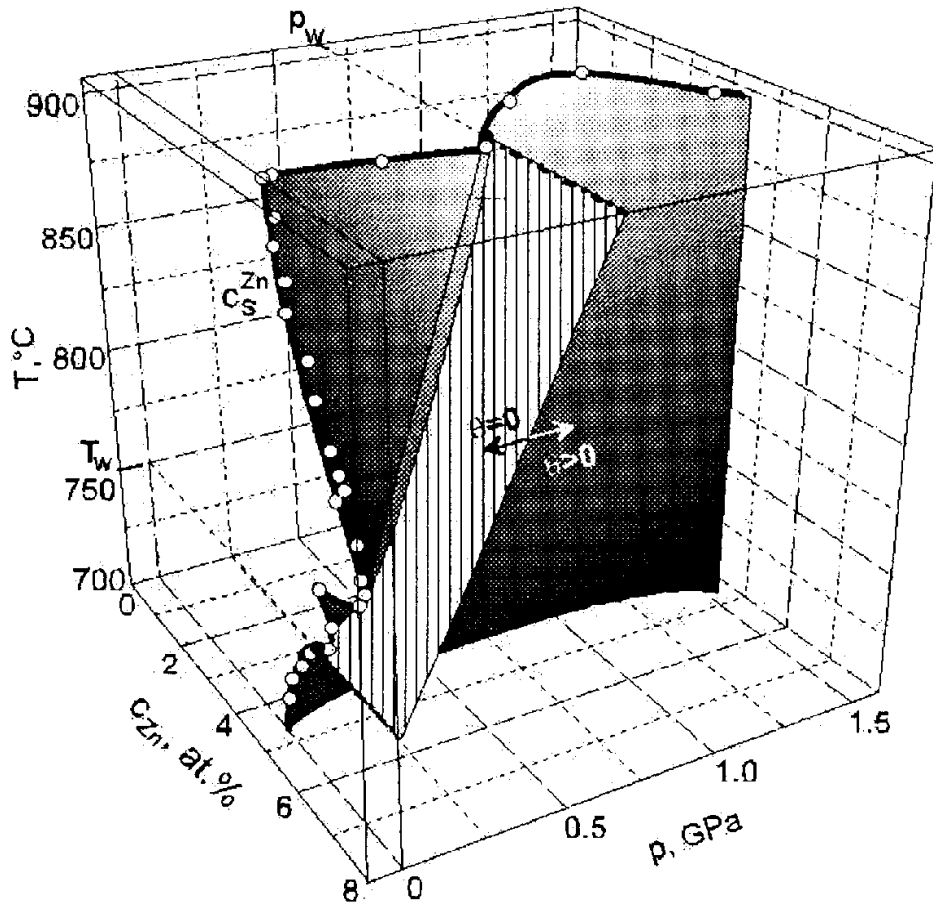


Figure 4. The three-dimensional phase diagram for the GB wetting transition of a $45^\circ\langle 001 \rangle$ GB in Fe-6 at.% Si alloy [36].

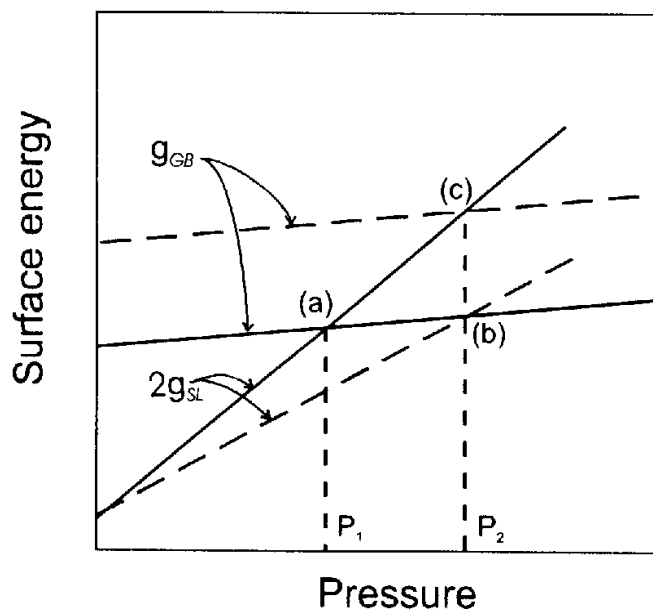


Figure 5. Schematic representation of the pressure effect on the energy of the S/L interface and GB.

The physical meaning of the dotted or dashed line in Fig. 3 and the fact that pressure has the strongest effect on the dewetting transition at the peritectic temperature was explained as follows [26, 35]. It was postulated that in the GB there are two types of clusters around the Zn atoms: the Γ phase clusters and the liquid-like clusters [26, 35]. The Γ -phase clusters are assumed to form below the peritectic temperature, where the Zn atoms may form bonds with Fe atoms like in the Γ phase which is the closest intermetallic phase. As the temperature increases up to the peritectic temperature the fraction of Γ phase clusters should decrease and the fraction of the liquid-like clusters should increase. On the other hand when approaching the melting point the fraction of liquid-like clusters should decrease at high temperatures because at high temperatures Zn is expected to desegregate from GBs. The above model explains the lowest solubility limit at the peritectic temperature. As a consequence, the higher the temperature the more solid-like the GB structure.

In conclusion: assuming that the energy of a liquid-like GB increases faster with pressure than a solid-like GB, the lowest dewetting pressure corresponds to the peritectic pressure. Further, it is expected that GBs should show a higher tendency towards premelting at intermediate temperatures, where low melting point impurities are still segregated on them, than at high temperatures, where desegregation takes place. This idea was expressed as solidification of GBs with increasing temperature [26] and corresponds to the bending to the right of the dashed and dotted lines in Fig. 3 describing the GB solubility limit, contrary to the behavior of the solid line which corresponds to the bulk solubility limit.

(c) *The effect of misorientation angle on the dewetting transition pressure.* As it is seen from Figs. 6 and 8, the dewetting pressure is highest for the near $\Sigma 5$ GB. Let us consider what that means. At low pressure, the GB is wetted and the equilibrium situation is when a liquid film separates the two grains. When the pressure is increased, the experimental fact is that the two crystals surfaces approach to each other and form the GB. Let us consider this situation based on the assumption that the intermediate state between wetting and dewetting is the formation of a thin liquid film corresponding to the prewetted state. The liquid film is stable to the highest pressure for the near $\Sigma 5$ GB. If the transition pressure is high, then either the GB energy is high or the excess volume of the liquid film is small (Fig. 5). It is unlikely that the near $\Sigma 5$ GB has a considerably higher energy than the general GBs. Therefore, the liquid film must have the smallest excess volume for the near $\Sigma 5$ GB (Fig. 5). It follows that for this periodic orientation of the two crystals, there must be some long range interaction of the crystals across the liquid phase, which decreases its excess volume. Such a situation would indicate that even in the prewetted state this near $\Sigma 5$ GB is not completely disordered.

(d) *The effect of pressure on the wetting angle.* Figure 8 shows the pressure effect on the wetting angle. Above the dewetting transition pressure the contact angle increases with pressure. We have performed a fitting procedure of Eq. (3) to the experimentally determined $\theta(p)$ dependencies. We used the following fixed values: $\gamma_{GB0} = 800 \pm 200$ mJ/m² and $\gamma_{SL} = 300$ mJ/m² [31,32, 64], $V_{GB} = 0$, and neglected the entropy terms. Using this procedure, the lower limit for the excess volume of the S/L interface was estimated: $V_{SL} > 0.2$ nm. V_{SL} is measured in the units: m³/m² = m. The results of the fitting procedure are listed in Table 1.

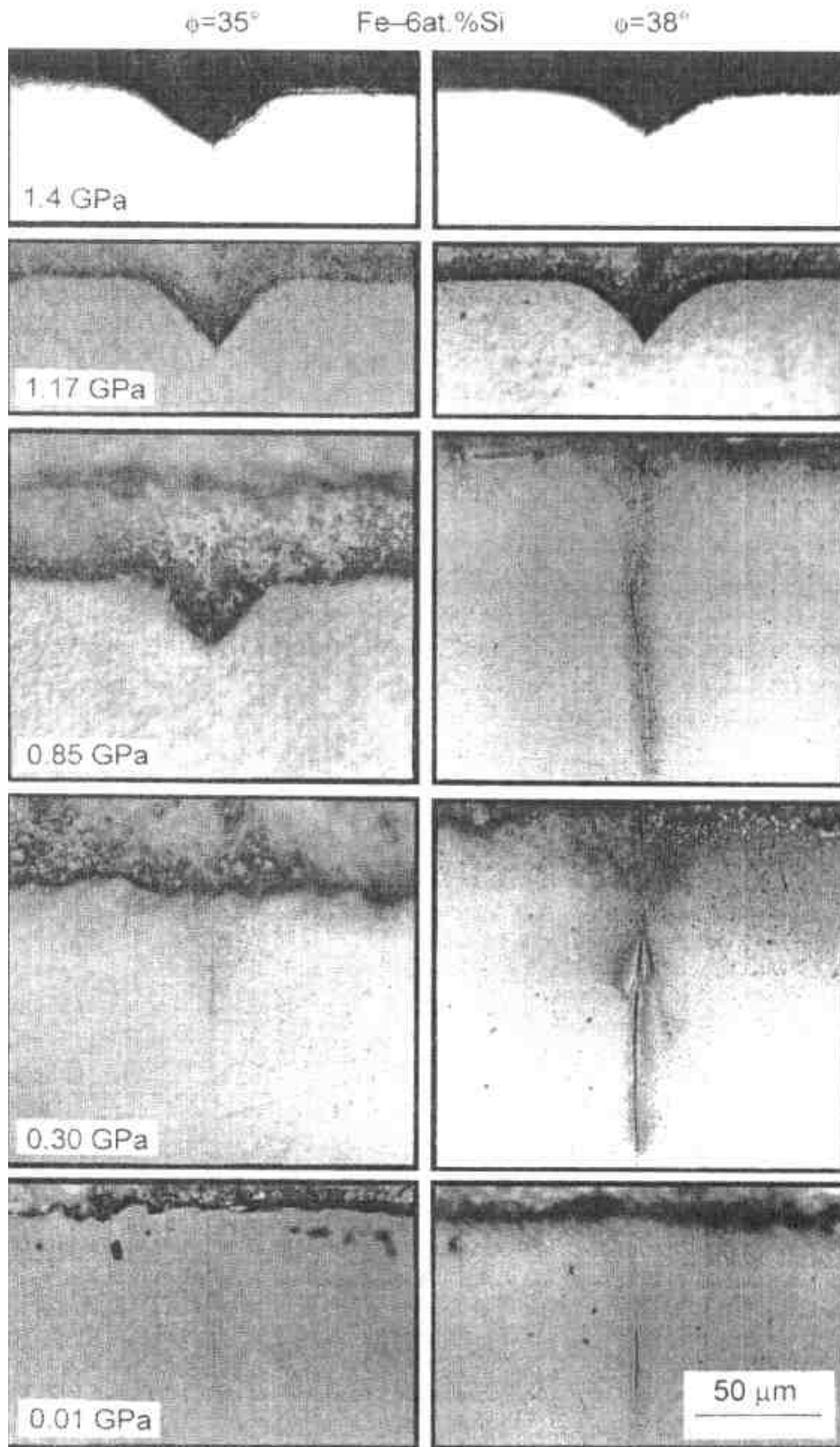


Figure 6. Optical micrographs of Fe(Si) bicrystals (below, bright) in contrast with a Zn rich melt (above, dark) after annealing at 905°C under different pressures. The GBs are represented by the thin vertical lines. The dewetting pressure is between 0.3 and 0.85 GPa for the 35°<001> symmetrical tilt GB while it is between 0.85 and 1.17 GPa for the 38°<001> near $\Sigma 5$ GB.

Table 1. Results of the fitting procedure of Eq. 3 to the experimental data shown in Fig. 8.

Misorientation angle	Dewetting pressure, GPa	V_{SL} , nm
35°	0.6 ± 0.1	0.65±0.15
38° (~Σ5)	0.8 ± 0.1	0.9±0.3
43°	0.4 ± 0.1	0.3±0.1

From thermodynamic considerations [45–49] and computer modeling studies [65–69] it follows that in the case of a low heat of fusion the S/L interface is diffuse and assumes a thickness of a few atomic diameters. However, such effects could not account for the high free volume found in the present study. In ref [36, 72] it was assumed that the S/L interface is thick by a few nm and the density deficit of the S/L interface originates from the fact that the liquid is less dense than the solid. Figure 9 illustrates the above concept. If the interface width L decreases to zero, the volume of the system decreases by $V_{SL} = L\Delta\rho$. The density difference $\Delta\rho$ between the liquid and solid is on the order of 2%. Therefore, for the minimum value of V_{SL} 0.2 nm, the S/L interface thickness is on the order of 10 nm. Such a thick S/L interface can be understood in terms of the association model of liquid alloys [70]. It predicts the stability of solid like-clusters in the liquid. If solid-like clusters containing a few atoms and of diameter 1–2 nm detach from the solid and dissolve in the liquid, then the S/L interfacial region must be at least a few nm thick. The above model was called melting iceberg model for the solid/liquid interface.

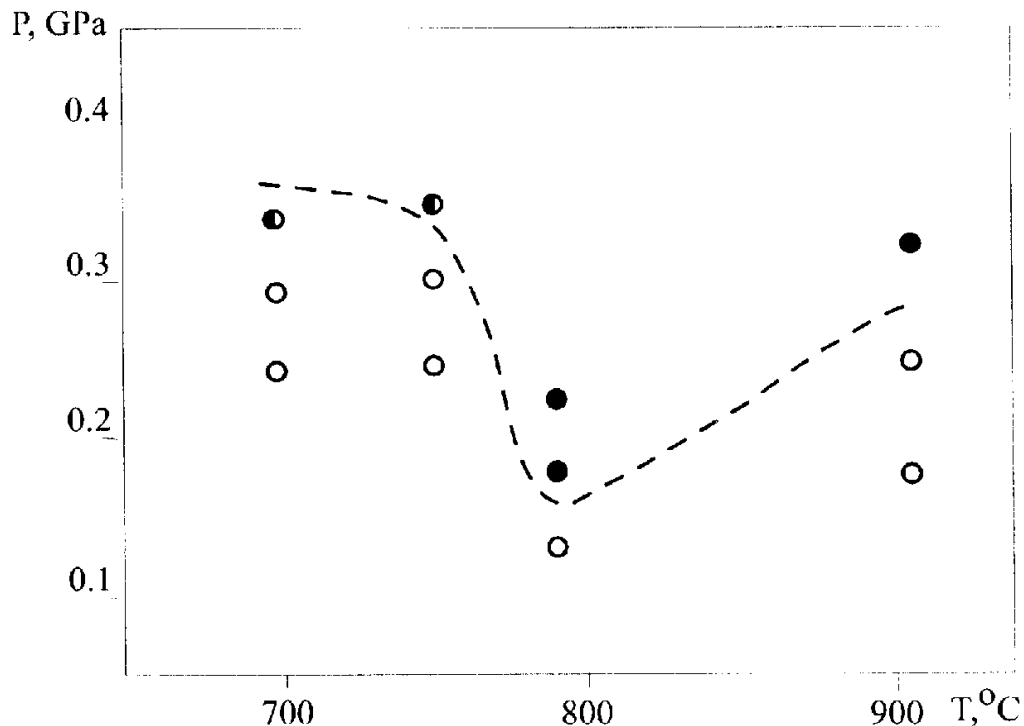


Figure 7. The effect of temperature on the dewetting pressure in Fe-6at.%Si bicrystals wetted by liquid Zn.

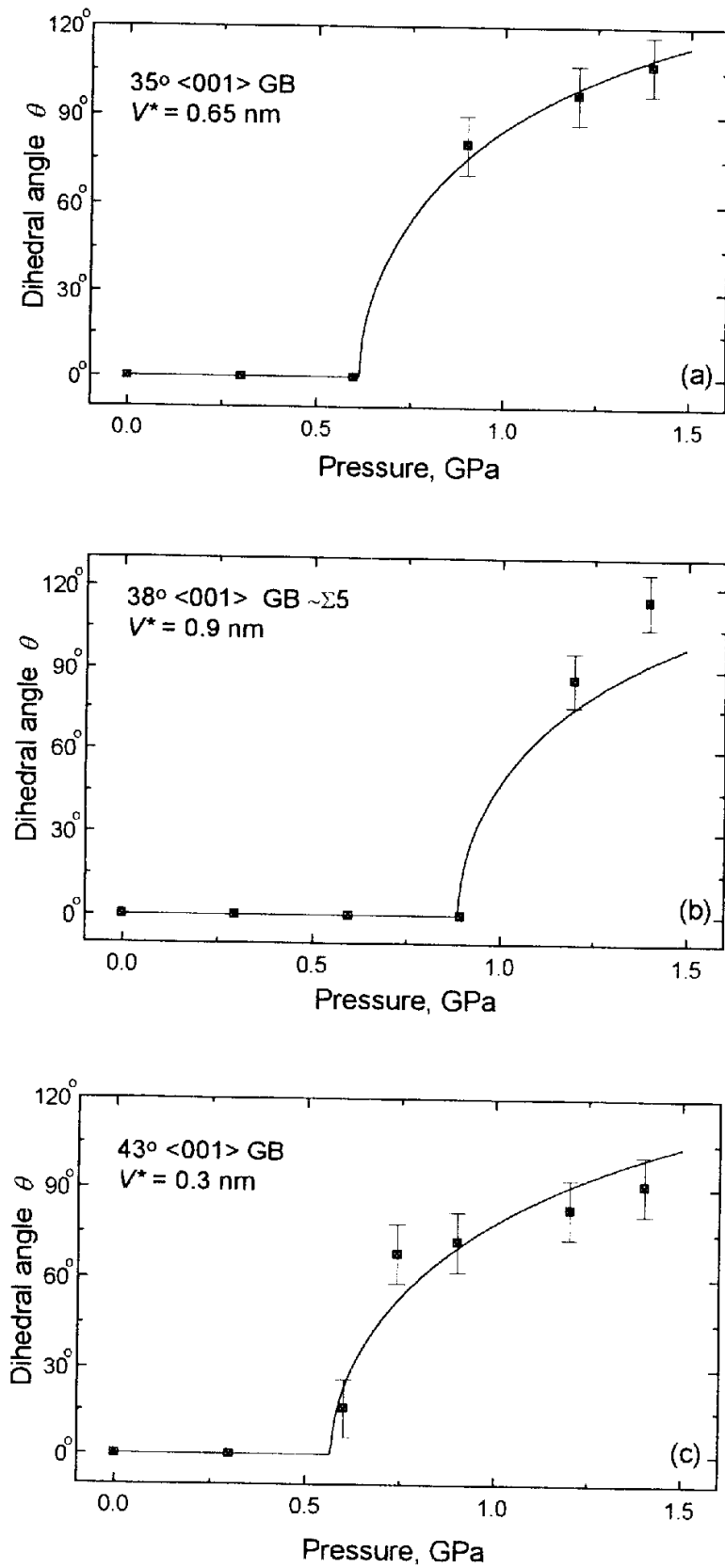


Figure 8. Pressure effect on the wetting angle for $<001>$ boundaries having a misorientation angle of 35° (a), 38° (b) and 43° (c). The calculated curves correspond to the best fit values for V_{SL} to Eq. 3.

The high excess volume of the S/L interfaces found in the present study was in contrast with the low excess volumes found by Stickels and Hucke [28] in the Ni–Pb system. However, these authors studied a system in thermodynamic equilibrium, where no interdiffusion perpendicular to the interface took place. In the case of Fe–Si bicrystals wetted by Zn, diffusional fluxes take place and the S/L interface has a reactive character. This may be the main reason of the difference in the behavior of the two systems under pressure.

The present results are also consistent with recent investigations of the pressure effect on GB segregation of oxide phases in ceramics [37]. It is known that such oxide layers may exist in thermodynamic equilibrium in GBs in ceramics [73]. However, application of high pressures may prevent both segregation and formation of amorphous GB films [37].

Conclusions

1. Pressure causes the de-wetting transition in Fe–6 at.% Si bicrystals by liquid Zn.
2. The strong pressure effect on the wetting angle indicates an excess volume of the solid/liquid interface in the above system of more than 0.2 nm.
3. To explain such a high excess volume, it was proposed that the S/L interface encloses clusters of atoms detaching from the solid and melting in the liquid, like in the case of melting icebergs. The above model was called the melting iceberg model for the solid/liquid interface.
4. The dewetting transition pressure is higher for the near $\Sigma 5$ special grain boundary than for the general boundaries. This result was interpreted as an evidence that the liquid film between two S/L surfaces is in that case not fully disordered.

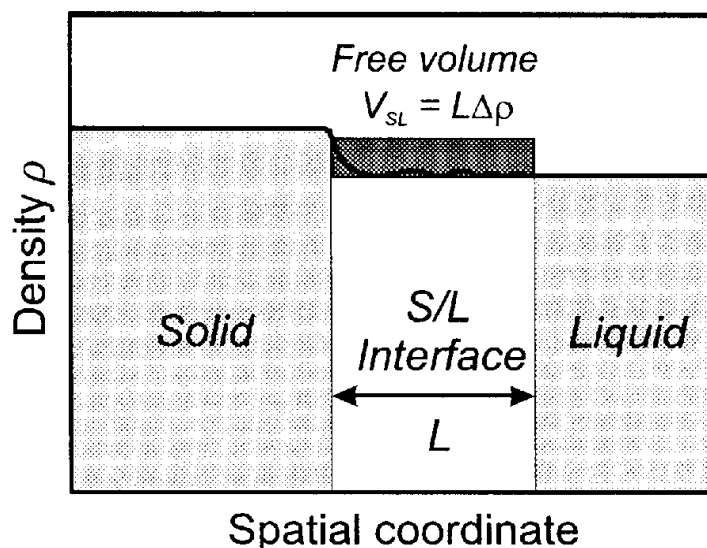


Figure 9. Illustration of the melting iceberg model for the solid/liquid interface. It is assumed that the S/L interface has density oscillations corresponding to solid-like atomic clusters which detach from the bulk and dissolve in the liquid. The width of the interface corresponds to the range of the existence of the clusters. If the interface width L decreases to zero, the volume of the system decreases by $V_{SL} = L\Delta\rho$. The absolute value of the change of volume per unit surface is defined as the excess volume of the S/L interface.

Acknowledgements This work was supported by the Polish Academy of Sciences, the TRANSFORM Program (BMFW 03N9004), and the NATO HTECH.LG.970342 grant.

References

1. G. W. Bolling and W. C. Winegard, *Acta Metall.* **5** (1957) p.681.
2. M. E. Glicksman and C. L. Vold, *Acta Metall.* **15** (1967) p.1409.
3. W. M. Robertson, *Trans. Metall. Soc. AIME* **233** (1965) p. 1232.
4. W. M. Robertson, *J. Appl. Phys.* **42** (1971) p. 463.
5. G. H. Bishop, *Trans. Metall. Soc. AIME* **242** (1968) p. 1343.
6. B. C. Allen, *Trans. Metall. Soc. AIME* **245** (1969) p. 1621.
7. H. J. Vogel and L. Ratke, *Acta Metall. Mater.* **39** (1991) p. 641.
8. D. R. Clarke, *J. Amer. Ceram. Soc.* **70** (1987) p. 15.
9. A. Otsuki and M. Mizuno, *Suppl. Trans. Jap. Inst. Metals.* **27** (1996) p. 789.
10. J. A. Kargol and D. L. Albright, *Metall. Trans. A8* (1977) p. 27.
11. M. Gündüz and J. D. Hunt, *Acta Metall.* **37** (1989) p. 1839.
12. A. Passerone and R. Sangiorgi., *Acta Metall.* **33** (1985) p. 771.
13. A. Passerone, R. Sangiorogi and N. Eustathopoulos, *Scripta Metall.* **16** (1982) p. 547.
14. G. Rao, D. B. Zhang and P. Wynblatt, *Acta Metall. Mater.* **41** (1993) p. 3331.
15. N. Eustathopoulos, *Int. Met. Rev.* **28** (1983) p. 189.
16. E. B. Evans, M. A. McCormick, S. L. Kennedy, and U. Erb, *Appl. Phys. A* **42** (1987) p. 269.
17. W. A. Kaysser, S. Takajo, G. Petzow, *Acta Metall.* **32** (1984) p. 115 and S. Takajo, Ph.D. Thesis, Dep. of Chemistry, University of Stuttgart (1981).
18. B. S. Bokstein, L. M. Klinger, and I. V. Apikhtina, *Mat. Sci. Eng. A203* (1995) p. 373.
19. V. N. Semenov, B. B. Straumal, V. G. Glebovsky, and W. Gust, *J. Crystal Growth* **151** (1995) p. 180.
20. E. I. Rabkin, V. N. Semenov, L. S. Shvindlerman, and B. B. Straumal, *Acta Metall. Mater.* **39** (1991) p. 627.
21. B. Straumal, T. Mushik, W. Gust, and B. Predel, *Acta Metall. Mater.* **40** (1992) p. 939.
22. B. Straumal, W. Gust, and D. A. Molodov, *Interface Science*, **3** (1995) p. 127.
23. B. B. Straumal, W. Gust, and D. Molodov, *J. Phase Equilibria* **15** (1994) p. 386.
24. L. S. Shvindlerman, W. Lojkowski, E. I. Rabkin, and B. B. Straumal, *Coll. Physique* **51**, C1- (1990) p. 629.
25. E. I. Rabkin, W. Gust, W. Lojkowski, and V. Paidar, *Interface Sci.* **1** (1993) p. 201.
26. W. Lojkowski and B. Palosz, *Mater. Res. Soc. Symp. Proc.* **357** (1995) p. 337.
27. B. Straumal, E. I. Rabkin, W. Lojkowski, and W. Gust, *Acta Mater.* **45** (1997) p. 1931.
28. C. A. Stickels and E. E. Hucke, *Trans. Metall. Soc. AIME* **230** (1964) p. 20.
29. F. M. d'Heurle and O. Thomas, *Defect Diff. Forum* **129-130** (1996) p. 137.
30. J. M. Howe, in *Interfaces in Materials*, (John Willey & Sons, Inc. New York, 1997), p. 219.
31. V. Missol, *Energies of Interfaces in Metals* (Slask, Katowice, 1975), p.32.
32. L. E. Murr, *Interfacial Phenomena in Metals and Alloys* (Addison - Wesley, London, 1975).
33. W. Lojkowski, U. Söderval, J. Swiderski, S. Mayer, W. Gust, B. Predel, and A. Lodding, *Trans. Mater. Res. Soc. Japan B* **16**, (1994) p. 1485.
34. W. Lojkowski, *Defect Diff. Forum* **129-130** (1996) p. 269.
35. W. Lojkowski, E. Rabkin, B. Straumal and W. Gust, *Defect Diff. Forum* **143-147** (1997) p. 1407.

36. B. Straumal, E. Rabkin, W. Lojkowski, W. Gust and L. S. Shvindlerman, *Acta Mater.* **45** (1997) p. 1931.
37. J.-R. Lee, Y.-M. Chang, G. Ceder, *Acta Mater.* **45** (1997) p. 1247.
38. H. Rogerson, J. C. Borland, *Trans. of the Metallurgical Soc, AIME* **227** (1963) p.2.
39. A. R. E. Singer and S. A. Cottrell, *J. Inst. Metals* **73** (1947) p. 33.
40. W. S. Pellini, *Foundry* **80** (1952) p. 124.
41. A. Rozenberg, M. C. Flemings and H. F. Taylor, *Modern Castings*, **7** (1960) p. 508.
42. T. Watanabe, S. Shima and S. Karashima. in "*Embrittlement by Liquid and Solid Metals*" Proceedings of The Metall. Society of AIME, (St. Louis, October 24, 1982), p.161 and 173
43. T. Watanabe, M. Tanaka and S. Karashima, *ibid*, p.183.
44. P. Berthier, F. LeGuyadre, J. Bernardini and M. Biscondi, *Defect Diff. Forum*, **143-147** (1997) p. 1541.
45. J. Woodroof, "*The Solid-Liquid Interface*", (Oxford Press, London 1974).
46. J. W. Christian, "The Theory of Transformations in Metals and Alloys", (1973), p.158.
47. J. E. Hillard and J. W. Cahn, *Acta Metall.* **6** (1958) p. 772.
48. W. A. Miller and G.A. Chadwick, *Acta Metall.* **15** (1967) p. 607.
49. D. Turnbull, *Trans. Metall. Soc. AIME* **221** (1961) p. 422.
50. T. E. Hsieh and R. W. Balluffi, *Acta Metall.* **37** (1989) p. 1637.
51. F. Carrion, G. Kalonji and S. Yip, *Scripta Metall.* **17** (1983) p. 915.
52. P. Giccotti, M. Guillope and V. Pontikis, *Phys. Rev.* **B 27** (1983) p. 5576.
53. P. Deymier, A. Taivo and G. Kalonji., *Acta Metall.* **35** (1987) p. 2719.
54. J. Q. Broughton and G. H. Glimer, *Phys. Rev. Letters*, **56** (1986) p. 2692.
55. H. Gleiter, *Z. Metallkd.* **61** (1970) p. 282.
56. S. Nichols and P.J. Levis, *Scr.Met.* **11** (1977) p. 491.
57. R. Kikuchi, J. W. Cahn, *Phys. Rev.* **B21** (1989) p. 1893.
58. Siu-Wai Chan, J. S. Liu, R. W. Balluffi *Scripta Metall.* **19** (1985) p. 1251.
59. W. Lojkowski, H. Gleiter and R. Maurer, *Acta Metall.* **26** (1988) p. 69.
60. U. Erb and h. Gleiter, *Scripta Metall.* **13** (1979) p. 61.
61. W. Lojkowski, unpublished results.
62. C. Roques-Carmes, M. Aucouturier and P. Lacombe, *Metal Sci. Journal* **7** 128 (1973).
63. D. Wolf and K.L. Merkle, in *Materials Interfaces*, edited by D. Wolf and S. Yip (Chapman & Hall, London, 1992), p.87.
64. A.R. Miedema and F. J. A. den Broeder, *Z. Metallk.* **70** (1979) p. 14.
65. A. Bonissent and B. Mutaftschiev, *Phil. Mag.* **35** (1977) p. 65.
66. J. M. Howe, *Phil. Mag. A* **74** (1996) p. 761.
67. F. Spaepen, *Scripta Metall.* **10** (1976) p. 257.
68. F. Spaepen, *Solid State Phys.* **47** (1994) p. 1.
69. G. Busnell-Wye and J. L. Finney, *Phil. Mag.* **44** (1981) p. 1053.
70. F. Sommer, *Z. Metallk.* **73** (1982) p.72 and 77.
71. A. P. Sutton, R. W. Balluffi, *Interfaces in Crystalline Materials*, (Clarendon Press – Oxford 1995), p.272.
72. W. Lojkowski, E. Rabkin, B. Straumal and W. Gust, submitted to *Interface Science*.
73. D. R. Clarke, *J. Am. Cer. Soc.* **70** (1986) p.15.